

Timing Analysis of the Light Curve of the Dipping-Bursting X-ray Binary X1916-053

Y. Chou, J. E. Grindlay, and P F. Bloser

*Harvard-Smithsonian Center for Astrophysics,
60 Garden Street, Cambridge, MA 02138
yichou@cfa.harvard.edu*

yichou@cfa.harvard.edu

ABSTRACT

We present the timing analysis results for our observations of the x-ray dip source X1916-053 conducted with RXTE between February and October of 1996. Our goal was to finally measure the binary period - as either the x-ray dip period or $\sim 1\%$ longer optical modulation period, thereby establishing if the binary has a precessing disk (SU UMa model) or a third star (triple model). Combined with historical data (1979-96), the x-ray dip period is measured to be 3000.6508 ± 0.0009 sec with a 2σ upper limit $|\dot{P}| \leq 2.06 \times 10^{-11}$. From our quasi-simultaneous optical observations (May 14-23, 1996) and historical data (1987-96), we measure the optical modulation period to be 3027.5510 ± 0.0052 sec with a 2σ upper limit $|\dot{P}| \leq 2.28 \times 10^{-10}$. The two periods are therefore each stable (over all recorded data) and require a 3.9087 ± 0.0008 d beat period. This beat period, and several of its harmonics is also observed as variations in the dip shape. Phase modulation of x-ray dips, observed in a 10 consecutive day observation, is highly correlated with the ~ 3.9 d dip shape modulation. The 1987-1996 optical observations show that the optical phase fluctuations are a factor of 3 larger than those in the x-ray. We discuss SU UMa vs. triple models to describe the X1916-053 light curve behavior and conclude that the x-ray dip period, with smaller phase jitter, is probably the binary period so that the required precession is most likely similar to that observed in SU UMa and x-ray nova systems. However the “precession” period stability and especially the fact that the times of x-ray bursts may partially cluster to occur just after x-ray dips, continue to suggest that this system may be a hierarchical triple.

Subject headings: accretion, accretion disks — stars: individual (X1916-053) — x-rays: stars

1. INTRODUCTION

The discovery of periodic (~ 50 min) dips in the x-ray flux from the moderately faint source 4U1915-05 (X1916-053) provided the first direct evidence for a binary periodicity in an x-ray burst

source (Walter et al 1982, White and Swank 1982). Combined with the general success of the thermonuclear flash model for (Type I) x-ray bursts (e.g. Joss and Li 1980), this confirmed that bursters are indeed neutron stars accreting from binary companions. The x-ray dips are believed to be caused by partial occultation by vertical structure (or clouds) in the accretion disk. The short dip period (~ 3000 sec), if identified as the binary period, provided the the first example of an ultra-compact x-ray binary with a very low mass degenerate companion.

The x-ray period has been reported with values from 2985 to 3015 sec (Walter et al. 1982; White and Swank 1982; Small et al. 1989; Yoshida et al. 1995 and Church et al. 1997). Smale et al. (1989) discovered a possible second candidate period of 2984.6 ± 6.8 sec from the Ginga 1987 observations. In addition to the primary dips, secondary dips with phase difference $\sim 180^\circ$ are sometimes observed. The varieties of dip width, depth, phase, and association with the period show the complex behavior of X1916-053. In addition to the 3000sec dip period, a 199d long-term x-ray modulation period was also reported by Priedhorsky and Terrell (1984).

The optical counterpart of X1916-053 was discovered (Grindlay et al. 1988) as a $V=21$ mag optical star with a modulation period of 3027.5 sec, $\sim 1\%$ longer than the X-ray dip period. The difference between the x-ray and optical periods leads to the question of which represents the orbital period of the system. The optical period was found to be stable over (at least) 7 years (Callanan, Grindlay and Cool, 1995, hereafter CGC95).

In this paper, we briefly introduce SU UMa vs. triple system models previously suggested (Grindlay, 1992) for explaining the x-ray/optical period difference (section 2), describe our 1996 RXTE observations of X1916-053 (section 3) and report (section 4) the timing analysis of the data, including the x-ray dip periodicity, ~ 3.9 d period dip shape modulation, the dip phase jitter phenomenon, and the long term x-ray dip period stability from the combination of the RXTE and previous x-ray observations (Einstein (1979-1981), EXOSAT (1983) and Ginga (1987-1990)). Analysis of our optical May 14-23, 1996, optical observations quasi-simultaneous with RXTE and historical (1987-96) optical data are used to derive the optical ephemeris and phase jitter for comparison with the x-ray values. We use the x-ray dip ephemeris, which is able to predict dip times within ~ 0.1 phase (300sec) back to 1979, to study the relation of the times of x-ray bursts to dips since a possible correlation was previously noted (Grindlay 1992). In section 5, we discuss SU UMa vs. triple models for the complex light curve behavior of X1916-053, concluding that either model would require interesting new phenomena to explain the present data but that the triple model would be required if the dip-burst correlation is real.

2. SU UMa and Triple Models

Grindlay (1989, 1992) pointed out that two models might account for the the beat behavior and the $\sim 1\%$ difference of the optical and the x-ray periods. The dual periods suggest either a SU UMa type precession or a triple system. SU UMa binaries are a subclass of dwarf novae, which

during their superoutburst state, display “superhumps” with periods a few percent longer than the orbital period (see, e.g., Warner 1995). Similar $\sim 1\%$ longer periods are formed in the optical outbursts of x-ray transients. For both SU UMa dwarf novae and x-ray transients, the binary period is the shorter of the two, and the longer period (which changes during outburst decay) is the beat between the binary and a longer disk precession period. Applied to X1916-053, the shorter x-ray dip period would be the binary period. Whitehurst (1988) has discovered by hydrodynamic simulation that an accretion disk in a CV system with a low-mass secondary is tidally unstable and leads to a precessing eccentric disk. Hirose and Osaki (1990) have derived the dependence of the disk precession period on binary mass ratio which we apply to X1916-053 in section 5.1.

The triple model for X1916-053 was proposed by Grindlay et al. (1988) and Grindlay (1989, 1992) to account for the apparent stability of the (longer) optical period and the reported 199d long-term modulation (Priedhorsky and Terrell 1984). Mazeh and Shaham (1979) showed that in a hierarchical triple system, the eccentricity of the inner binary is modulated at a long-term period $P_{long} = KP_{out}^2/P_{in}$, where P_{in} and P_{out} refer to the binary period and the orbital period of the third companion and K is a constant of order unity which depends on mass ratios and relative inclinations. Under the triple model, the third companion period (~ 4 d) in the X1916-053 system should be the beat period of the x-ray dip period and the optical period. X-ray dips are due to mass transfer “surges”, from the change in inner binary eccentricity induced by third star at the period given by the beat between the outer and inner orbital periods. If the optical period, the longer one, is the binary period, then this triple companion is in a retrograde orbit and the constant K=0.46 for X1916-053 system. This model also predicts that the x-ray dips should display phase glitches (Bailyn 1987) and a timing correlation between x-ray dips and x-ray bursts (Grindlay 1992, and see section 4.4).

3. RXTE and Optical 1996 OBSERVATIONS

RXTE Observations of X1916-053 were made from 1996 February to October. A $\sim 10^4$ sec (~ 3 orbit) observation of X1916-053 was conducted about once per month except March and April. Between May 14 to 23, the observations were made about once per day. The observation details and mean count rates (outside dips and bursts) are given in Table 1. A total of 37 complete primary dips (hereafter, dips) and 4 secondary dips with various depths and dip duration were recorded. A typical light curve is shown in Figure 1. All observations except two contained dips. No dip was observed in the May 5 observation due to Earth occultation. However, for the May 15 data, two dips did not appear at the expected times (see Figure 2).

The data used for analysis is the PCA (PCU 0 and 1) Standard-2 data with time resolution 16 sec. We divide the data into 4 energy bands, 1.72-3.18keV, 3.18-5.01keV, 5.01-6.84keV and 6.84-19.84 keV. Since the energy dependence is small in the dip centroid-timing analysis (see, e.g. Church et al. (1998)) for analysis of spectral variation in dips for X1916-053), we only present the analysis results for band 4 unless specified. A complete analysis of the persistent source (outside

dips) spectra and variations of X1916-053 for these RXTE observations is presented by Bloser et al (2000).

Optical observations of X1916-053 were carried out (by PFB) from 1996 May 14 to 23, with the Mt. Hopkins 48-inch Telescope with a broad-band B+V filter. The exposure time of each optical image was 300 sec, but RXTE visibility constraints prevented the observations from being exactly simultaneous. The magnitude of X1916-053 for each exposure was measured with DAOPHOT (Stetson, 1987) relative to the average magnitude of several nearby stars. A reference star close (~ 1 arcmin) to X1916-053 and within ~ 1 mag was used to measure the total measurement errors of the observation. Some data are not included in the analysis because of the large fluctuation in the comparison star. Only five nights' observations (UT May 15, 16, 20, 21 and 23) have good light curves for analysis. A typical optical light curve is shown in Figure 3.

4. DATA ANALYSIS

We first describe a period folding analysis for an initial determination of the x-ray dip period. This is then refined, and limits on \dot{P} are derived from the phase analysis. We then apply a similar analysis for the optical data and derive, similarly, a long-term ephemeris. Finally, we use the dip ephemeris to examine the dip phase of x-ray bursts detected from X1916-053.

4.1. X-ray Dip Periodicity Analysis

All data were initially corrected for arrival times at the solar system barycenter. We first carried out a χ^2 analysis of the folding light curves (32 bins) to search for the best period of X1916-053 dips near 3000 sec for the entire 1996 RXTE data. The maximum χ^2 is at 3000.6 sec as shown in Figure 4. Fitting the 3000.6 sec peak with a Gaussian gave the best period of 3000.625 ± 0.192 sec. The side bands are mainly the results of the beat period of observation gaps.

Performing the same χ^2 analysis on the ten consecutive observations in May, we find that there is a family of peaks, in addition to the 3000 sec peak, including a 3026.23 ± 3.23 sec peak near the 3027 sec optical variation period. The centroid of these peaks associated with the 3000 sec period implies that there is a modulation with a fundamental period of ~ 3.9 days, as previously noticed (Grindlay 1992), in the X1916-053 x-ray light curves (see Figure 5). If we take the modulation period to be the 3.9087d beat period of the optical period (3027.5510 sec; cf. section 4.3) and the x-ray dip period (3000.6508 sec; cf. section 4.2) respectively, we may then define the x-ray side band periods as

$$\frac{1}{P_n^{side}} = \frac{1}{P_x} - \frac{n}{P_m} \quad (1)$$

where $P_x = 3000.6508$ sec, $P_m = 3.9087$ d, $n = \pm 1, \pm 2, \dots$ and P_m/n is the n th harmonic of the

modulation period. Table 2 shows the expected side band periods and the measured side band periods.

To further study the origin of the ~ 3.9 d beat period, we folded the light curves with the folding period of 3000.625 sec for each of ten consecutive days. The daily folded light curves are grouped into 4 day groups in Figure 6 to demonstrate the light curve variations. The ~ 3.9 d period is evident as variations in dip shape, especially duration. In Figure 6, the first column (May 14, 18 and 22) has the largest dip widths, and the width narrowed in the following 3 days (except May 15 when, surprisingly, no dip was observed). The second row (May 18 to 21) of the plot shows a complete period of the width variations. On the last day of each cycle (May 17 and 21), the secondary dips appear so that these are also tied to the ~ 3.9 d clock. The dip depths also have a variation period of ~ 3.9 d (see Figure 6) but the change is not as significant as the variation in the dip widths.

Schmidtke (1988) reported two possible optical periods of 2924.76 ± 2.1 sec and 3027.48 ± 2.2 sec in observations from the CTIO 1.5m telescope on UT 1987 May 3, 4, 5 and 8. Table 2 suggests that the 2924.76sec period is probably an observation of the harmonic index -3 side band. Grindlay (1989 and 1992) reported that the x-ray period was found in the optical light curves also. Together with the side bands and dip width-intensity modulation, we now find in the RXTE x-ray light curves, the reality of a stable ~ 3.9 d period in the X1916-053 system is now established.

4.2. X-ray Dip Phase Analysis

We use the phase of the dip center time folded by a trial ephemeris to refine the dip period, measure the phase variations, update the ephemeris and derive the period derivative. The dip center time is obtained from fitting a quadratic curve around the minimum of the dip and then folding it with a trial period and an arbitrary but fixed start epoch as the phase zero.

The phase analysis can be used as an independent means to determine the best fit period in addition to the folding light curve analysis in section 4.1. The first trial period may be taken arbitrarily but must be close to the true period so that there is no cycle count ambiguity for neighboring observations. We choose the period from a χ^2 analysis of all 1996 light curves to be the initial trial period. The slope of the linear fit of the phase Φ and dip center time for the data obtained over time interval t gives the correction of the period as

$$\frac{\Delta\Phi}{t} = \frac{\Delta P}{P_{fold}^2} \quad (2)$$

We repeat the correction process until the phase drift rate (i.e. the slope) is much smaller than the error of the slope of the linear fit. Similar to the period correction, the error of the period is derived from the error of the fit slope. For the RXTE 1996 February to October data set, the best

period from a linear fit is 3000.625 ± 0.02 sec (see Figure 7) and the RXTE x-ray dip ephemeris can be written as

$$T_{RXTE} = MJD50123.00944 \pm 1.4 \times 10^{-4} + (3000.625 \pm 0.02)/86400 \times N \quad (3)$$

To further improve the accuracy of the x-ray dip period as well as to study the long term stability of X1916-053 period, we analyzed historical data. First, we folded the dip center times of Ginga '87, '88, and '90 observations (cf. Yoshida et al 1995) with eq.(3). Together with the RXTE observations, we found a phase drift with a constant rate, which implies that a constant period can phase all the 1987-1996 data. The period error of 0.02 sec in eq.(3) is equivalent to a phase error of 0.07 per year. The probability of cycle count ambiguity can be written as (assuming the distribution is Gaussian)

$$Prob = \int_{-0.5}^{0.5} [1 - \exp(-\frac{\Phi^2}{2\sigma^2}) / \sum_{n=-\infty}^{\infty} \exp(-\frac{(\Phi + n)^2}{2\sigma^2})] d\Phi \quad (4)$$

The 0.07 phase error per year gives the probabilities of cycle count ambiguities 0.007, 0.027 and 0.199 for the '87 to '88, '88 to '90 and '90 to '96 data, respectively.

We divide the RXTE observations into two parts, the first and the second halves of 1996. Together with the Ginga '87, '88 and '90 observations, we have a total of 5 data sets (all, of course, corrected to the barycenter). We take the average phase to be the mean phase of each dataset and assign the mean phase fluctuation to be the error of the phase. The linear fit for the Ginga-RXTE data refines the dip period to be $P = 3000.6508 \pm 0.0021$ sec.

Next, we add the Einstein '79-'81 data (Walter et al. (1982) and White and Swank (1982)) and EXOSAT '83 data (Smale et al. (1988)), again all barycenter corrected, and fold with the 3000.6508 sec period and the ephemeris of eq.(3). In the EXOSAT data sets, folding the dip center times with the ephemeris above to the 1985 May and October data (3 dips) yields phase of 0.48 ± 0.02 . Thus these are secondary dips and are excluded from further analysis. We assign a ± 0.05 phase error from the phase jitter range to each dataset. The x-ray ephemeris can phase all of the 1979-1996 dataset within a phase error of ± 0.07 with no clear systematic derivative. The linear fit result shows that the phase drift rate is 2.19×10^{-6} per day, which is smaller than the phase drift error 8.37×10^{-6} per day (1σ). Hence, no period correction is necessary for the x-ray ephemeris and the best fit x-ray dip ephemeris (hereafter, the x-ray ephemeris) is:

$$T_{dipcenter} = MJD50123.00944 \pm 1.4 \times 10^{-4} + (3000.6508 \pm 0.0009)/86400 \times N \quad (5)$$

The quadratic fit of Φ vs. t gives the period derivative because

$$P(t) \approx P_0 + \dot{P}t = P_{fold} + \Delta P + \dot{P}t \quad (6)$$

Thus, the phase can be written as

$$\Phi \approx \Phi_0 + \frac{\Delta P}{(P_{fold})^2} t + \frac{1}{2} \frac{\dot{P}}{(P_{fold})^2} t^2 \quad (7)$$

where P_{fold} is the folding period, $\Delta P = P_0 - P_{fold}$ and Φ_0 and P_0 are constants. The X1916-053 x-ray dip period derivative from a quadratic fit for all 1979-1996 data sets is

$$\frac{\dot{P}}{P} = (6.50 \pm 10.86) \times 10^{-8} \text{ yr}^{-1} \quad (8)$$

The minimum χ^2 fit gives χ^2 values of 2.00 and 1.64 and a reduced χ^2_ν of 0.286 and 0.274 for linear and quadratic fits, respectively. From the one sided F-test, we obtain $F = \Delta\chi^2/\chi^2_{\nu,quad} = (2.0 - 1.64)/0.274 = 1.31$ in the comparison of linear and quadratic fits. Thus the quadratic fit, shown in Figure 7, is not significantly better than the linear fit. We derive a 2σ (90%) confidence level upper limit for any change in the x-ray dip period as $|\dot{P}_{x-ray}| \leq 2.06 \times 10^{-11}$.

When the dip centers of the RXTE 1996 May data are folded by the x-ray ephemeris (shown in Figure 9), a phase systematic variation is clearly seen on the time vs. phase plot. In the RXTE 1996 May observations, the phases form two groups. The dips from May 16, 17 and 21 have phases larger than 0 and all the others (except May 15, with missing dips) smaller than 0. The range of the phase jitter is about ± 0.05 in phase. The phase jitter seems to have some correlation with the 3.9d period. We fit a 50% duty cycle square wave with fixed 3.9087d period (the beat period of x-ray and optical periods). The minimum χ^2 fit result is shown as Figure 9 and the reduced χ^2 is 0.45 for 19 degrees of freedom.

Yoshida (1993) and Yoshida et al.(1995) fit the dip phase variation with a sinusoidal period 6.5 ± 1.1 d from Ginga 1990 September observations, so we did a similar analysis for the RXTE 1996 May observations. There are two (local) χ^2 minima between the periods of 3.0d to 7.0d, 4.85 ± 0.12 d and 3.76 ± 0.10 d, with amplitudes of ~ 0.06 phase (or ~ 3 min) and reduced χ^2 's 0.49 and 0.60, respectively (17 degrees of freedom). Both fits are good. However, although the 3.76 ± 0.10 d period result has slightly larger reduced χ^2 , it is consistent with the 3.9d phase jitter, or the dip width modulation period. The sinusoidal fit with fixed period of 3.9087d gives a reduced χ^2 of 0.69 (18 degrees of freedom). All the fit results are shown in Figure 9. Thus the 3.9d period found for the dip phase modulation with RXTE is also within $\sim 1\sigma$ of 0.5 the Ginga period (since $3.9 \sim 0.5(6.5 + 1.1)$).

4.3. Analysis of optical light curves

The stability of the optical modulation period is critical for us to decide which model best describes the X1916-053 system. The optical period was confirmed by CGC95 to be stable over 7

years and the times of minima can be described by a simple ephemeris. We have now found the x-ray period to be stable for ~ 17 years (see section 4.2). Both periods have comparable long-term stability with significantly different period values. However, in the long-term stability analysis in Grindlay (1989), CGC95 and section 4 of this paper, the minimum phases are averaged over several days to several months. Those long-term analyses ignore the short-term phase fluctuations (say, several days). Figure 10 shows the X1916-053 phase distribution of both x-ray and optical 1987-1996 observations folded by the corresponding ephemerides for x-ray (eq. (5)) and optical (from CGC95) data respectively. The mean phase of the x-ray dips is 0.00098 with 1σ fluctuation of 0.06, and none of the 101 dips exceeds phase ± 0.2 . On the other hand, the optical minima have a mean phase of 0.0573 and 1σ fluctuation of 0.151 using the CGC95 optical ephemeris. This shows that the optical minima have larger fluctuations than the x-ray dips. The ~ 0.05 offset in the optical minima phases is correction of the phase zero epoch given by CGC95 that is required to fit the 1996 optical data.

With the new dataset of 1996 observations, the long-term stability of X1916-053 optical modulation can be tested again. We folded the light curves by the optical ephemeris from CGC95 for each night's observation to obtain the minimum phase of the night. The same method described in section 4.2 is applied to get the average minimum phases and the average observation times for each dataset. We assigned 0.15 phase error obtained from the mean fluctuations in phase to each dataset. The linear fit shows that the optical ephemeris results in a phase drift of 5.07×10^{-6} per day with 1σ error of 4.93×10^{-5} per day. Correction of the period from CGC95 is unnecessary because the phase drift is less than the error. The linear fit demonstrates that the ephemeris in CGC95 is still good but we have obtained a smaller error of the period at 5.23×10^{-3} sec ($= 6.06 \times 10^{-8}$ d) than the one in CGC95 ($= 8 \times 10^{-8}$ d). Incorporating the 0.05 phase offset, we derive the final X1916-053 optical ephemeris

$$T_{optmin} = HJD2444900.0046 \pm 0.003 + (3027.5510 \pm 0.0052)/86400 \times N \quad (9)$$

From the quadratic fit, we obtain a period derivative of

$$\frac{\dot{P}}{P} = (8.9 \pm 11.88) \times 10^{-7} \text{ yr}^{-1} \quad (10)$$

which could be ~ 14 times larger than that from the x-ray dips but again is not a significant detection of \dot{P} . Both linear and quadratic fits yielded good fits with small reduced χ^2 values of 0.169 and 0.106 respectively. The F value of the one-side F-test is 6.3 for comparison of the linear fit and the quadratic fit. This value implies that the quadratic fit, as shown in Figure 11., is better than the linear fit at the $\sim 95\%$ confidence level. The 2σ (90%) confidence level upper limit for the change in optical period is $|\dot{P}_{opt}| \leq 2.28 \times 10^{-10}$

4.4. Analysis for Triple Model

Grindlay et al. (1988) and Grindlay(1989,1992) proposed a triple model in which the third star period was related to the beat period of optical and x-ray periods (~ 3.9 d). In a hierarchical triple, the predicted (Bailyn 1987) phase of the minima of the inner binary separation, and thus (potentially) the mass transfer rate \dot{m} would be modulated at the beat between the outer (~ 3.9 d) and inner binary (3000 sec) periods. The x-ray dips are due to these \dot{m} modulations which “puff up” the accretion ring (where the accretion stream strikes the inner disk). So that dips do not occur at a preferential inner binary phase.

Bailyn (1987) shows that the phase of the inner binary separation should “glitch” twice per outer orbit, so we expect corresponding phase jumps in x-ray dip times. Indeed the possible square wave modulation of x-ray dip phase (Figure 9) is suggestive. However, the observed dip phase modulation is about a constant x-ray dip period, whereas the phase glitches expected (Bailyn 1987) in the inner binary separation and thus dip times are additive: they effectively delay the times of dips so that over the outer orbit period there are as many total minima (dips) as there are inner binary orbits. Thus the x-ray dip phase should not depart from the binary phase by more than ~ 0.5 (depending on the “glitch spacing ratio”, in turn dependent on outer vs. inner binary mass ratio). On the other hand, if the x-ray and optical clocks are independent, their relative phase offsets (on either the x-ray or optical ephemeris) will be randomly spaced. Thus, the free running x-ray and optical phases folded by the “wrong” period (e.g., folding the optical minima with x-ray ephemeris or folding the x-ray dips with optical ephemeris), will make the phase offsets drift linearly. If the observation times are random, the phase difference will be random and give rise to a uniform (with certain statistical fluctuation) dip (or minimum) phase difference distribution. Grindlay (1992) found marginal evidence from the 1990 Ginga and optical data for correlated optical minima vs. x-ray dips.

We therefore analyzed the phase difference of the simultaneously-observed optical minima and x-ray dips. A total of 12 pairs of (x-ray and optical) dips/minima in the '87-'96 datasets (9 primary and 3 secondary dips/minima) have dip-center/minimum time differences less than 1500 sec and can thus be compared in phase for the same binary orbit. Figure 12 shows the phase difference distribution of these quasi-simultaneous dips/minima. Doing a simple χ^2 analysis for phase differences gives a reduced χ^2 of ~ 1 when folded by either the x-ray or optical ephemeris. Both phase differences are thus consistent with a uniform distribution. Interestingly, though, the 3 secondary x-ray dips are clustered in a somewhat narrow phase range (-0.1 — +0.3); clearly a larger sample is needed.

The triple model makes one other prediction (Grindlay 1992) : that there may be an association between x-ray dips and x-ray bursts. This is because each accretion surge (resulting in a dip), occurring at the dip period of successive minimum separation times, enhances the probability of a nuclear flash at times just following. The dip, due to obscuration by enhanced material and clumps in the accretion ring, precedes the flash by the timescale required for it to accrete from the ring onto

the NS. This must be small, since the mean height of the ring must decay promptly (in the triple model) for the dips to have their observed typical duration of ~ 0.1 - 0.2 phase. This then suggests the ring empties out, and accretes, via an ADAF flow (Narayan and Yi 1995) since the viscous timescale for accretion in a thin disk from the ring at $R \sim 10^8$ cm in this ultra-compact LMXB would still be ≥ 3000 sec, or at least a full binary period. Therefore if accretion onto the NS is enhanced by the rapid decay of the ring, perhaps through quasi-spherical accretion, the probability of the accreted material reaching the critical density to flash is expected to be greatest for times just after a dip.

In Figure 13 we show the phase distribution of 41 x-ray bursts as recorded by OSO-8, EXOSAT, Ginga and RXTE when folded on our final x-ray dip ephemeris (with phase 0 the phase of primary dips). One third of the bursts concentrate in phase 0-0.2 (after primary dip). The distribution has a χ^2 probability of 0.006 of being random (flat). The binomial probability of detecting 17 bursts in the “interesting” phase interval ~ 0 — 0.2 (required to match typical dip durations (cf. Figure 6) and thus enhanced accretion time) relative to the uniform distribution (8 bursts) is 0.016. No such effect is seen if the burst times are folded on the optical period (dashed line in Figure 13).

5. DISCUSSION

Table 3 shows all the x-ray dip periods reported since 1982. The side bands from the RXTE analysis of X1916-053 may explain the many different reports of the x-ray dip periodicity of X1916-053. Owing to the insufficient time span of the observations, both uncertainties of the 3000 sec period peak and its first neighbor side bands are large such that the peaks merge to affect the centroid of the 3000 sec peak. The centroid shifts left or right depending on which (first left or right) side band is more significant.

The analysis in this paper suggests that there is a ~ 3.9 d period modulation in the dip width and depth, and the phases may also have a ~ 3.9 d period jitter with an amplitude of 0.1 (peak-to-peak). The 6.5 ± 1.1 d period for dip phase reported by Yoshida et al. (1995) is probably the sub-harmonic of 3.9d period. The optical modulation also has a ~ 4 d period in amplitude, and possibly phase modulation (Grindlay 1992), which is consistent with our RXTE x-ray observations.

The fact that both the x-ray and the optical light curves have the ~ 3.9 d beat period implies that there are 3 periodicities in the X1916-053 system, with periods of approximately 3000 sec, 3027 sec and ~ 3.9 d. Of these three periodicities, at most two of them are independent because of the beat relation among them. One of the two short (3000 sec and 3027 sec) periods should represent the binary orbital period and it should be the more stable one. Both the optical and the x-ray period have long-term stabilities over the total historical data span of ~ 9 years and ~ 17 years respectively. The period derivative of the optical modulation could be ~ 14 times larger than that for the x-ray dips, although both \dot{P} values are statistically insignificant. The phase jitter statistics show that the x-ray dips have smaller fluctuations than the optical minima. Thus the x-ray dip

period may be the better candidate for the orbital period, and thus X1916-053 contains a precessing disk as in SU UMa systems. However, the larger optical phase jitter could simply be due to the shallower modulation in the optical vs. x-ray (compare Figure 3 and Figure 6).

As outlined in section 2, SU UMa and triple models have been proposed to explain the $\sim 1\%$ difference of x-ray dip and optical variation periods. We consider additional implications of each model.

5.1. SU UMa Model Implications

Our result that the x-ray dips have less phase jitter, and are at least (if not more) stable over the historical database, provides strong support for the SU UMa model. Applying the SU UMa model to the X1916 system, the 3000 sec x-ray dip period is the orbital period which is due to the shadow of accretion stream which crosses our line of sight ~ 0.1 in binary phase before the secondary star. The 3027 sec optical period (the “superhump” period) is due to the beat with the 3.9d precession period of accretion disk. The asymmetric disk and its ~ 3.9 d retrograde precession that changes the vertical structure (cloudlets) at the outer edge with ~ 3.9 d period, provide an explanation for the 3.9d modulation of x-ray dip shape and phase.

Hirose and Osaki (1990) performed hydrodynamic simulations of accretion disks for the superhump phenomenon in SU UMa stars. They showed that the disk precession angular frequency can be written as

$$\frac{\omega_p}{\omega_{orb}} = a(r) \frac{q}{(1+q)^{1/2}} \quad (12)$$

where

$$a(r) = \frac{1}{4} \frac{1}{r^{1/2}} \frac{d}{dr} \left(r^2 \frac{db_{1/2}^{(0)}(r)}{dr} \right), \quad (13)$$

q is the mass ratio, r is the ratio of disk radius and binary separation and $b_{1/2}^{(0)}(r)$ is the Laplace coefficient of order 0 in celestial mechanics (see Brouwer and Clemence 1961, equation 42, Chapter 15). Hirose and Osaki also demonstrated that the tidal instability of accretion disks is caused by the parametric resonance between particle orbits in the disk and the orbiting secondary star with 1:3 period ratio. Then, from Kepler’s third law, $r = (1/3)^{2/3} = 0.48$ for the tidal instability radius. From the Laplace coefficients in Brouwer and Clemence (1961), $a(r = 0.48) = 0.41$. Applying this model to the X1916-053 system, for which $w_p/w_{orb} = 0.0089$, the mass ratio is $q = 0.022$, or the mass of the secondary star $M_2 = 0.03M_\odot$ for the assumed $1.4 M_\odot$ neutron star. This compares favorably with the value $M_2 = 0.016M_\odot$ derived from the requirement that Roche lobe-filling secondary has $R_{WD} \sim R_{RL}$. Thus the secondary is indeed a helium white dwarf, as expected from its binary period.

The analysis in this paper indicates that the x-ray dip period is more likely to be the true orbital period, which supports the SU UMa model. The only problem may be the stability of the superhump period. The optical period derivative obtained by the 1987-1996 dataset is $|\dot{P}| < 2.28 \times 10^{-10}$, whereas the SU UMa stars typically have $\dot{P} \sim -(3-10) \times 10^{-5}$ (Patterson et al. 1993a). However, Patterson et al. (1993b) showed that the range of superhump period derivatives is $|\dot{P}| \sim 10^{-3} - 10^{-9}$ (for V795 Her, $|\dot{P}| < 1.7 \times 10^{-9}$, see Zhang et al. 1991).

AM CVn(=HZ 29), a binary with a white dwarf primary star and low mass helium white dwarf secondary star, is a compact binary system which has behavior similar to X1916-053. It has two¹ periods, 1028 sec and 1050 sec. Patterson et al. (1993c) discovered the 13.38 hr period, the beat period of the 1028 sec and 1050, in the helium absorption-line profile and suggested that its accretion disk is elliptical and slowly precesses around the white dwarf. Provencal et al. (1995) and Solheim et al. (1998) analyzed the Whole Earth Telescope (WET) data and discovered the 1051 sec period is very stable with period derivative of $\dot{P}(1051s) = +(1.71 \pm 0.04) \times 10^{-11}$ (~ 10 years baseline)². They concluded that 1051 sec is the orbital period and 1028 sec is the superhump period which would be opposite to the normal superhump system and not supported by the tidal instability model. On the other hand, Skillman et al. (1999) found that the period derivative of 1028 sec period is even more stable with $|\dot{P}(1028s)| < 2 \times 10^{-12}$ (over 7 years baseline). Thus, they concluded the shorter period is the orbital period and the longer one is the superhump period, which is comparable with our results for X1916-053. Both systems thus have very stable long-term superhump periods (\dot{P}_{sh} (AM CVn) = $+1.7 \times 10^{-11}$ and \dot{P}_{sh} (X1916-053) = $P_{opt} \times \dot{P}_{opt}/P_{opt} \sim +8.6 \times 10^{-11}$, $\sim 10^6$ times smaller than ones from typical superhumps of dwarf novae). Therefore, at least some of the “superhump CVs” (e.g. AM CVn, V795 Her³) have very stable superhump periods comparable to X1916-053.

The very stable superhump period implies a corresponding stable mean mass transfer rate, and thus x-ray luminosity. This is because conservative mass transfer (assumed) at rate \dot{M}_2 implies $\dot{P}/P = \dot{M}_2/M_2$ (van der Klis et al. 1993) where M_2 is the secondary star mass. Our limit (eq. (8)) implies that $\dot{M}_2 \leq 6.4 \times 10^{-9} M_{\odot} \text{yr}^{-1}$, or $L_x \sim 0.15 \dot{M}_2 c^2 \leq 5.4 \times 10^{37} \text{ erg/sec}$, which is a factor of ~ 10 larger than the typical system luminosity measured from our RXTE data (Bloser et al. 2000). Thus, measurement of $\dot{P}/P \sim 10^{-10}$, combined with measured variations in L_x on the ~ 190 d period (see below), might allow a conclusive test of the SU UMa model.

¹In fact, AM CVn also has a 1011 sec period which perhaps comes from the beat period of the 1028 sec period and a 16.96 hr nodal regression period (Patterson et al. 1993c, Skillman et al. 1999).

²The 1051 sec period wanders with $\dot{P} = \pm 2 \times 10^{-8}$ (time scale of 4-12 months) but the mean period has not wandered more than 0.1 sec in 35 years, which leads to $|\dot{P}| < 10^{-10}$ (Skillman et al. 1999).

³These are not true SU UMa (superhump) systems since neither system has been observed to have outbursts.

5.2. Triple Model Implications

Although the SU UMa (or superhump) model is the conservative choice, we cannot exclude the triple model (Grindlay et al 1988, Grindlay 1989) since it could also explain the reported (Priedhorsky and Terrell 1984; hereafter PT84) 199d long-term modulation of X1916-053 (cf. section 2).

We have searched for the \sim 199d period by an epoch-folding analysis. We find comparably significant peaks in a χ^2 vs. period plot at \sim 160d and 190d but not at the 198.6 ± 1.72 d value found by PT84. Longer epoch analysis for the 199d period is needed, since the \sim 4 yr RXTE/ASM data span is short enough that a “local” period departure of the Mazeh-Shaham period is possible (Mazeh, private communication). Extended x-ray and optical coverage is also needed to reduce the limits on \dot{P} for both the x-ray dip and optical periods. Although the predicted (Bailyn 1987) phase glitches for the x-ray dips, and the implied phase clustering of x-ray dips vs. optical (binary) minima, are not found in our phase analysis (except possibly for secondary dips), more simultaneous x-ray and optical observations are needed.

The strongest remaining evidence for the triple model is the surprising clustering of x-ray burst times vs. the times of x-ray dips (cf. Figure 13). This would be expected under the triple model if the enhanced matter in the accretion ring can be accreted very rapidly onto the NS: for bursts to occur within the \sim 0.2 phase bin following a dip, the accretion time must be \leq 600 sec. This itself would be almost as interesting as the retrograde triple system nature (and its origin; possibly in a globular cluster), since such a surprisingly short accretion timescales implies accretion via an ADAF-like quasi-spherical flow, rather than a dense accretion disk, from the ring down to the NS. Although the dip vs. burst association appears to be significant, more data are (as usual) needed. Quasi stable burst repetition times have been seen in one other source, GS1826-238 (Cocchi et al 2000), but without the remarkable stability apparent in X1916-053.

If the bursts are indeed correlated with dips (i.e. follow by \sim 0.0-0.2 phase), then under the simple binary and SU UMa model this would imply bursts are preferentially detected when the $\sim 0.03 M_\odot$ WD secondary is approximately aligned between us and the NS (i.e. when the NS would be eclipsed if the system were at higher inclination). We consider two very unlikely possibilities: lensing and beaming. The WD-NS alignment might suggest gravitational lensing or focusing small bursts on the NS otherwise not detectable. However, this would not preferentially amplify bursts since the accretion luminosity would be similarly lensed. The near-eclipse WD-NS alignment could imply burst emission is somehow beamed, perhaps by the WD-NS accretion stream-tube which might confine the burst at its footprint on NS by magnetic pressure. The lensing or beaming scenarios are both so implausible that confirmation of the burst-dip association would (virtually) require the triple model.

A final test of the triple vs SU UMa models could be made by irrefutably establishing the burst correlations (triple model) or spectroscopically showing that the dip period is the binary period

(SU UMa model).

The authors thank D. Barret, J. Halpern and T. Mazeh for discussions, K. Yoshida for provision of Ginga results and the HEASARC, from which archival OSO-8, EXOSAT and Ginga light curves were obtained for dips and bursts. This work was supported in part by NASA grant NAG5-3298.

REFERENCES

Bailyn C. D. 1987, *ApJ*, 317, 737

Bloser P. F., Grindlay J. E., Barret D. & Boirin L. 2000, *ApJ*, in press

Brouwer, D. & Clemence, G.D. 1961, *Method of Celestial Mechanics* (Academic Press, London)

Callanan, P. J., Grindlay, J.E. & Cool, A. M. 1995, *PASJ*, 47, 153 (CGC95)

Church, M. J., et al. 1997, *ApJ*, 491, 388

Church, M. J., et al. 1998, *A&A*, 338, 556

Cocchi, M. et al 2000, 5th Comp. Symp., AIP Conf. Proc., 510, 203

Frank, J., King, A. and Raine, D. 1992, *Accretion Power in Astrophysics*, Cambridge Univ. Press, p. 99.

Grindlay, J. E., Bailyn, C. D., Cohn, H., Lungger, P. M. Thorstensen, J. R. & Wegner, G. 1988, *ApJ*, 334, L25

Grindlay J. E. 1989, in Proc of the 23rd ESLAB Symposium on Two Topics in X-ray Astronomy, J. Hunt, B. Battrick, ed ESA SP-296, p121

Grindlay, J. E. 1992 in Proc. of the 28th Yamada Conference Frontiers of Astronomy, ed Y. Tanaka, K. Koyama (Tokyo), p69

Hirose, M. & Osaki, Y. 1990, *PASJ*, 42, 135

Hirose, M., Osaki, Y. & Mineshige, S. 1991, *PASJ*, 43, 809

Joss, P.C. and Li, F.K. 1980, *ApJ*, 238, 287

Mazeh, T. & Shaham, J. 1979 *A&A*, 77, 145

Narayan, R. & Yi, I. 1995 *ApJ*, 444, 231

Patterson, J., et al. 1993a, *PASP*, 105, 69

Patterson, J., et al. 1993b, *ApJS*, 86, 235

Patterson, J., et al. 1993c, *ApJ*, 419, 803

Priedhorsky, W. C. & Terrell, J. 1984, *ApJ*, 208, 661

Provencal, J. L., et al. 1995, *ApJ*, 445, 927

Schmidtke, P. C., 1988, *A.J.*, 95, 1528

Skillman, D. R., et al. 1999, *ASAP*, 111, 1281

Smale, A.P., Mason, K. O., White, N. E. & Gottwald, M. 1988, *MNRAS*, 232, 674

Smale, A.P., Mason, K. O., Williams, O. R. & Watson, M. G. 1989 *PASJ*, 41, 607

Smale, A. P., Mukai, K., Williams, O. R., Jones, M. H. & Corbet, R. H., 1992, *ApJ*, 400, 330

Solheim, J. -E., et al. 1998, *A&A*, 332, 939

Stetson P. 1987, *PASP* 99, 191

van der Klis, et al. 1993, *MNRAS*, 260, 686

Walter, F. M., Bowyer, S., Mason, K. O., Clarke, J. T., Halpern, J. & Grindlay, J. E. 1982, *ApJ*, 253, L67

Warner, B. 1995, *Cataclysmic Variable Stars* (Cambridge University Press)

White, N. E. Swank, J. H. 1982 *ApJ*, 253, L61

Whitehurst, R. 1988, *MNRAS*, 232, 35

Whitehurst, R., et al. 1989, *Proceedings of 23rd ESLAB Symposium*, vol.1, p127

Yoshida, K. 1993, Ph.D. Dissertation, Kanagawa University

Yoshida, K., Inoue, H., Mitsuda, K., Dotani & T Makino, F. 1995, *PASJ*, 47, 141

Zhang, E., et al. 1991, *ApJ*, 381, 534

Fig. 1.— A typical X1916-053 dipping light curve. The dashed lines are the expected dip center times for the ephemeris derived in section 4.2.

Fig. 2.— May 15th observation. No dip is observed at the expected dip center times (the dashed lines).

Fig. 3.— A typical optical (B + V band) light curve observed on UT 1996 May 20. The top one is the X1916-053 optical light curve and the dashed lines are the expected minimum times from the updated ephemeris given in eq. (9). The offset between expected and observed minimum times is due to the phase fluctuation. The bottom one is the light curve of a nearby comparison star for the identification of the observation confidence.

Fig. 4.— Result of folding period search for all RXTE X1916-053 1996 observations.

Fig. 5.— Result of the folding period search for RXTE X1916-053 data during ten consecutive days in 1996 May. The 3.9d beat side bands appear beside the dip period. The period of first side band on the right of the 3000 sec peak is close to the optical modulation period 3027.551 sec.

Fig. 6.— The folding light curves of the 10 consecutive day observation (14-23 May, 1996). All light curves are folded with a period of 3000.625 sec and an arbitrary but constant phase zero epoch.

Fig. 7.— Dip center time vs. phase of all RXTE X1916-053 1996 observations. The folding period is 3000.625 and the phase zero epoch is MJD50123.00944.

Fig. 8.— X-ray dip center time vs. phase of X1916-053 1979-1996 observations. The folding period is 3000.6508 sec and the phase zero epoch is MJD50123.00944. The dash line is the quadratic fit result.

Fig. 9.— Phase jitter of the RXTE X1916-053 1996 May observation. The solid line is the best square wave fit result (for $P = 3.9087$ d) and the dashed lines are the χ^2 minimum fit results (periods labeled) for sinusoidal phase delay variations.

Fig. 10.— X1916-053 phase distributions for x-ray dips (top) and optical minima (bottom) folded by the x-ray and optical ephemerides respectively. The optical minima show larger phase fluctuations.

Fig. 11.— Optical minimum time vs phase for X1916- 053 '87-'96 observations. The folding period is 3027.5510 sec and the phase zero epoch is HJD2446900.0046. The dashed line is the quadratic fit result, and the bars show the range of phase jitter for each observation.

Fig. 12.— Phase difference distributions of 12 pair quasi-simultaneous observed dips/minima on X1916-053. The plot on the top is the distribution of $\Delta\phi (= \phi_{opt} - \phi_x)$ folded by the x-ray ephemeris, and the bottom one is the distribution of $\Delta\phi (= \phi_x - \phi_{opt})$ folded by the optical ephemeris. The solid lines are the distributions for the 9 pairs of primary dips/minima and dashed lines are for the

3 pairs of secondary dips/minima.

Fig. 13.— Phase histogram for 41 x-ray bursts (OSO-8 through RXTE data) when folded on the x-ray dip ephemeris (primary dips at phase = 0, solid line). The burst arrival times appear to be clustered following primary and secondary dips. The dashed line is the phase histogram for x-ray burst when folded on the optical ephemeris. The burst arrival times are independent of the optical modulation.

Table 1. Journal of RXTE observations

Date dd/mm/yy	Start Time UT(hh:mm:ss)	Stop time UT(hh:mm:ss)	Time on Source (sec)	Mean Band 4 Count Rate (cts/sec)
10/02/96	00:14:18	05:09:36	9808	225.4
05/05/96	22:16:32	03:20:32 ^a	7280	96.42
14/05/96	09:22:08	12:55:44	8160	29.57
15/05/96	12:32:16	15:11:44	6880	43.60
16/05/96	12:56:48	16:31:44	8240	43.35
17/05/96	08:20:16	11:49:36	7872	37.54
18/05/96	09:53:52	13:20:32	7888	23.38
19/05/96	10:06:40	13:34:56	7920	24.48
20/05/96	06:50:24	10:16:32	7888	27.53
21/05/96	07:48:00	11:22:40	8400	24.69
22/05/96	12:38:08	16:26:40	8688	30.53
23/05/96	07:50:56	10:23:44	6912	71.01
01/06/96	17:37:04	21:36:32	9857	81.69
15/07/96	11:49:52	16:09:52	10144	63.22
16/08/96	10:37:52	14:55:44	10448	51.76
06/09/96	16:00:32	21:26:40	9936	71.89
29/10/96	06:53:36	11:22:40	9968	68.03

^aNext day

Table 2. Expected vs. observed side bands

Harmonic index	Expected side band period (sec)	Measured side band period (sec)	Error of measured side band period (sec)
1	3027.551	3026.23	3.23
2	3055.939	3053.50	2.93
3	3082.826	3081.53	3.41
4	3111.227	3109.11	4.24
-1	2974.224	2977.48	4.01
-2	2948.259	2950.39	2.85
-3	2922.743	2926.79	3.91
-4	2897.665	2901.12	2.89

Table 3. Measured X1916-053 x-ray dip periods

Mission	Time of obs (Year)	Period (sec)	Error (sec)	Reference
OSO-8	78	3003.6	1.8	1
		2995.8 ^a	3.6	1
Einstein	79, 80, 81	2985	10.0	2
EXOSAT	83, 85	3015	17.0	3
Ginga	87	3005.0	6.6	3
		2984.6 ^a	6.8	3
Ginga	87	3001.2	3.0	4
Ginga	89	2998.8	6.2	4
Ginga	90	3000.0	1.2	4
ACSA	93	3005	10	5
RXTE	96	3000.625	0.020	6
All	79-96	3000.6508	0.0009	6

^asecond candidate

References. — (1) White & Swank 1982; (2) Walter et al. 1982; (3) Smale et al. 1989; (4) Yoshida et al. 1995; (5) Church et al. 1997; (6) this paper

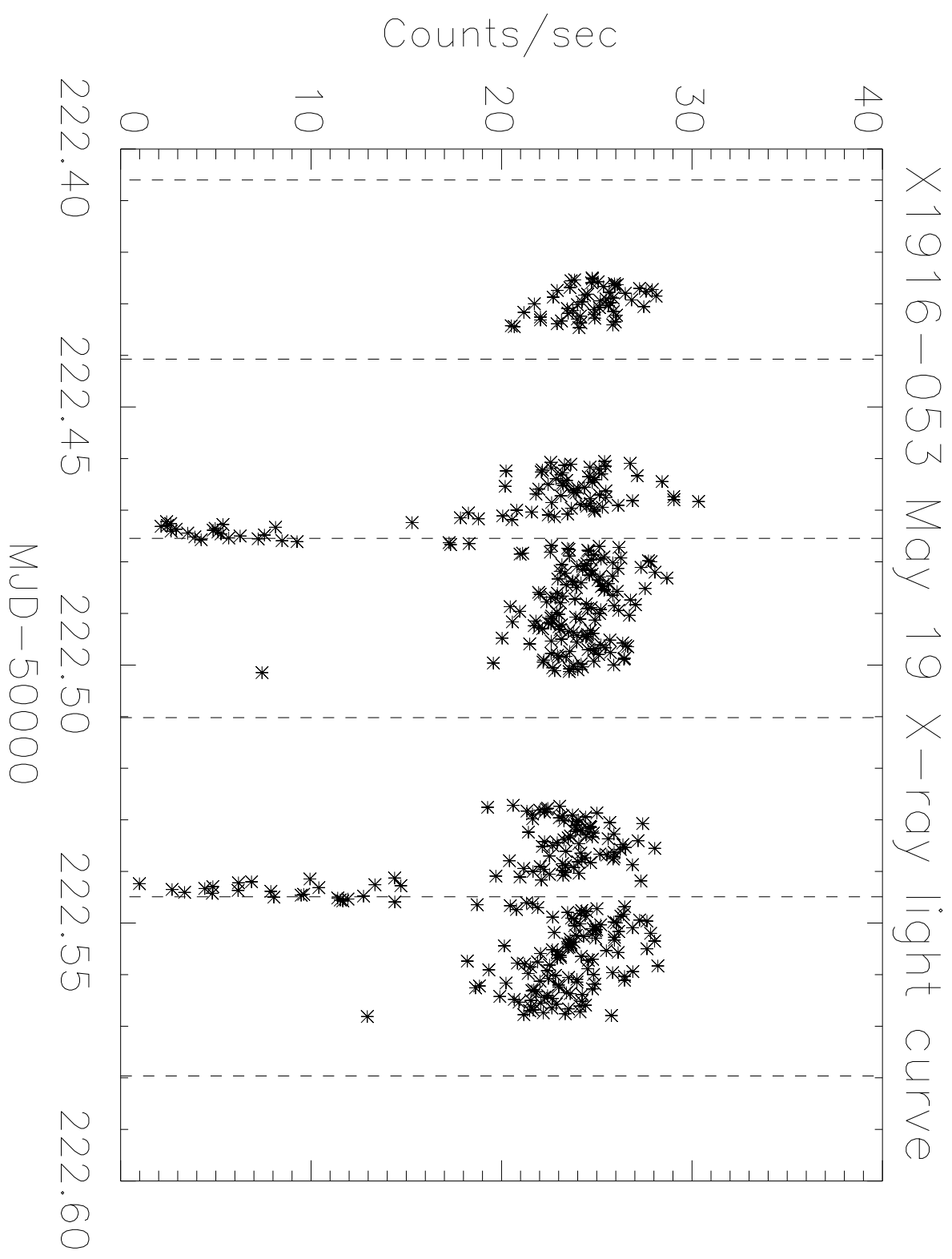


Fig. 1.—

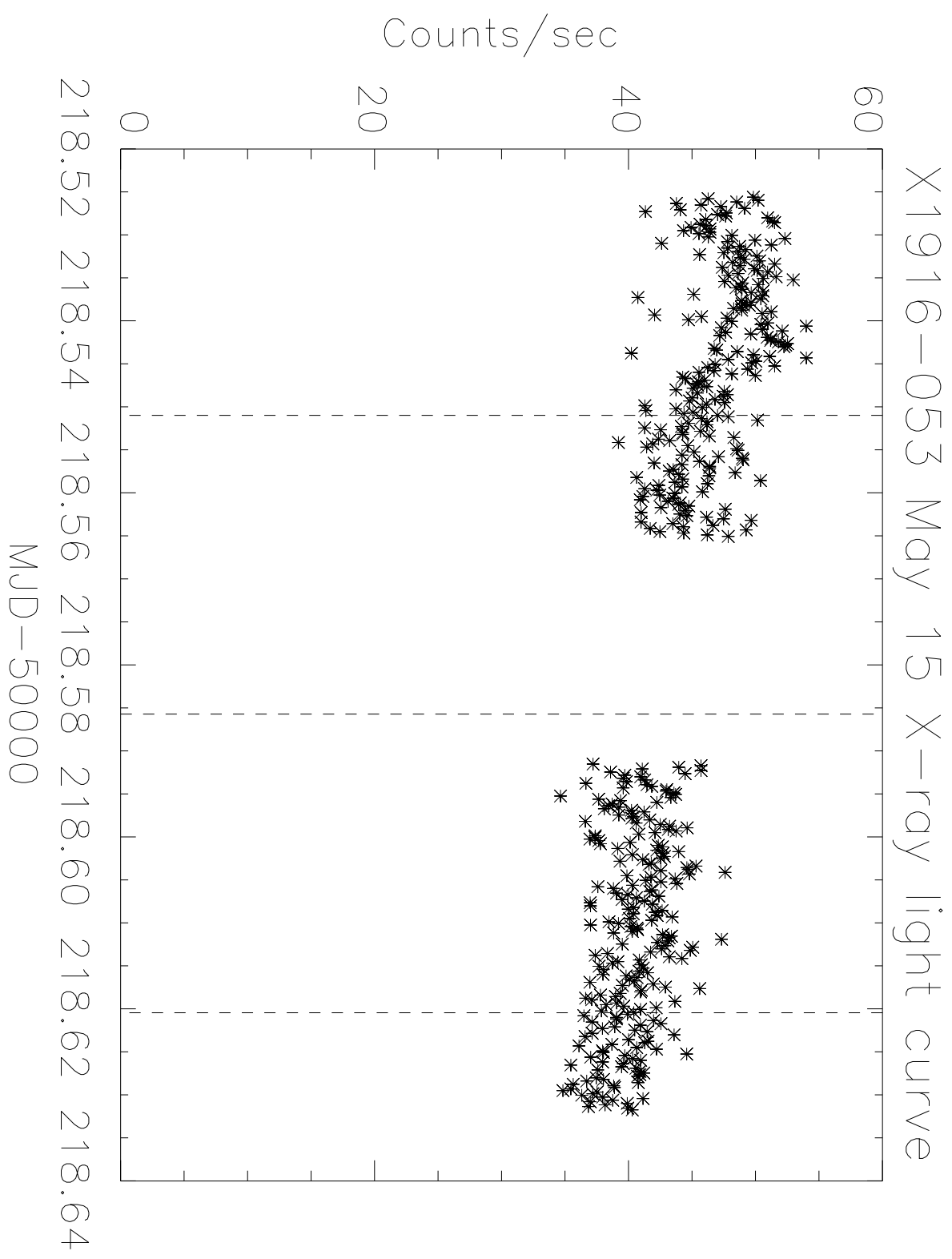
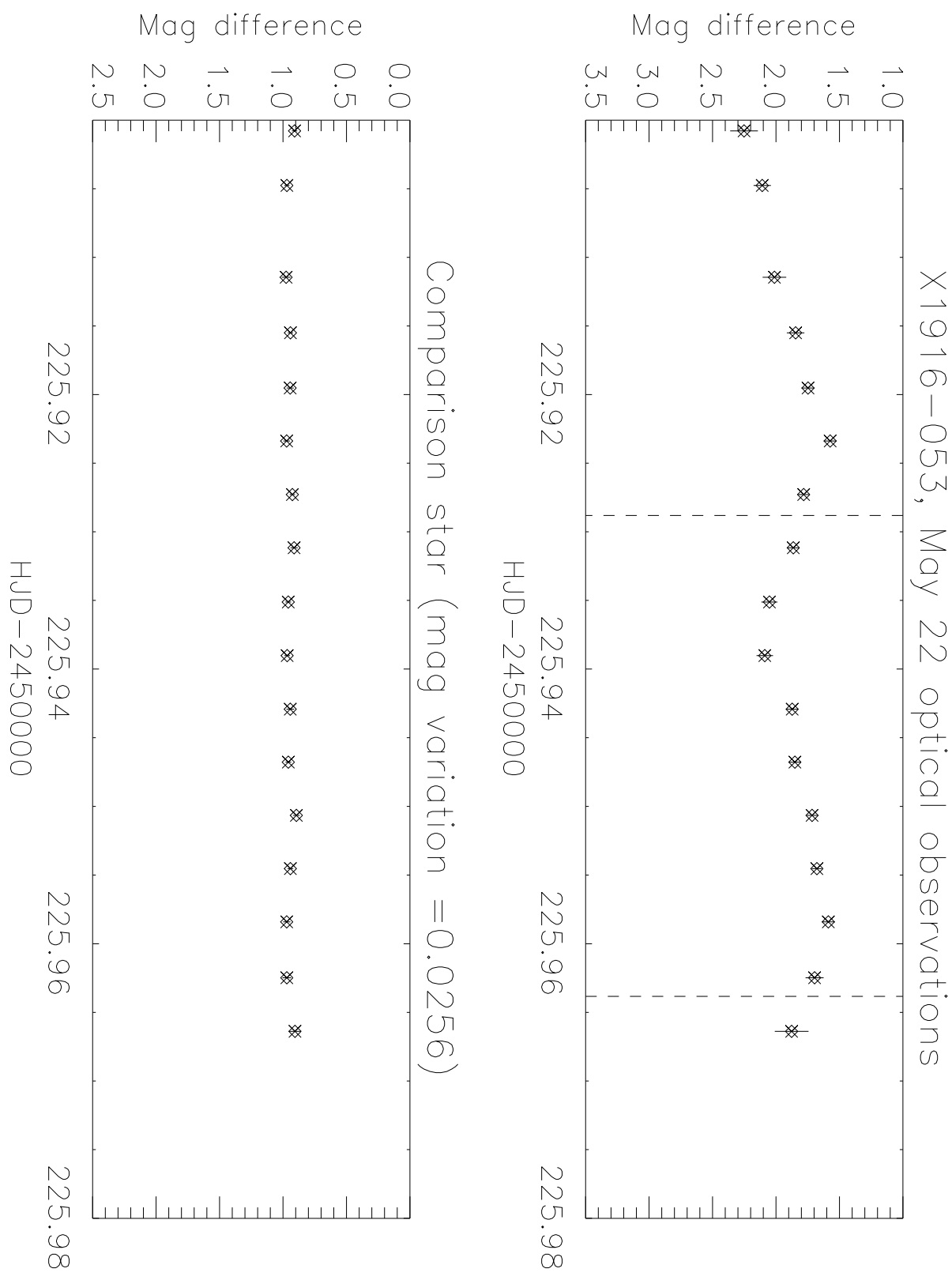


Fig. 2.—



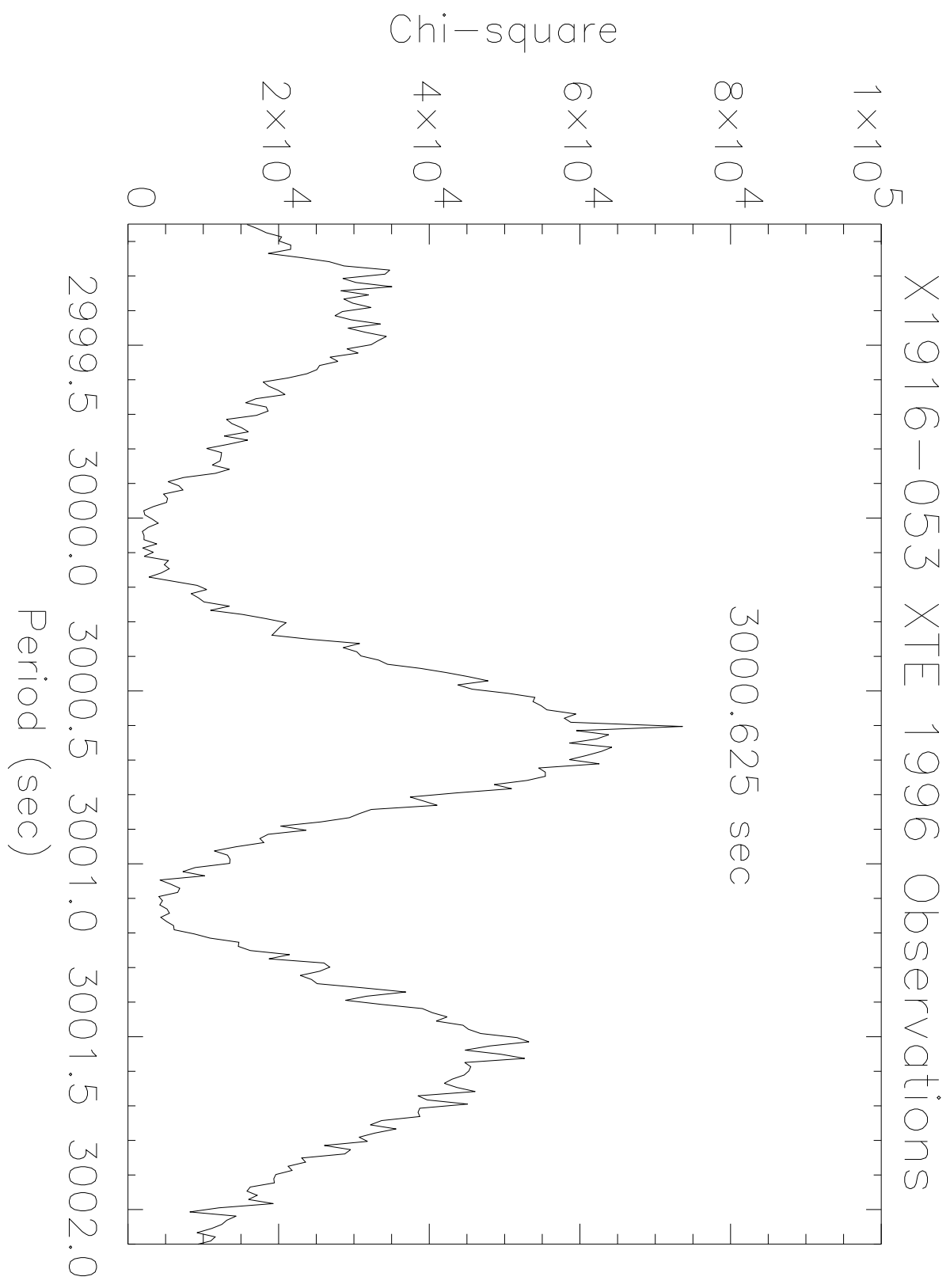


Fig. 4.—

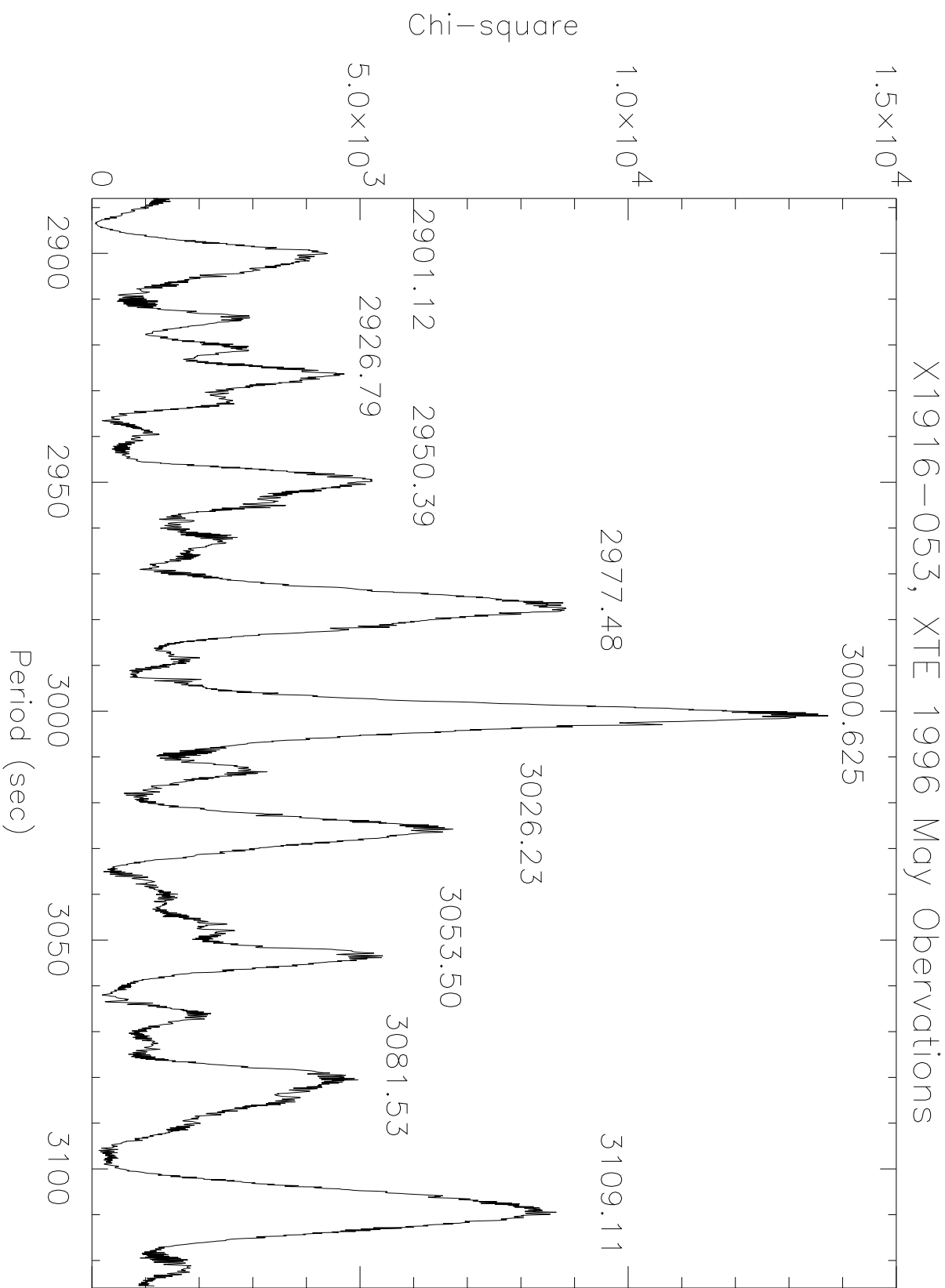


Fig. 5.—

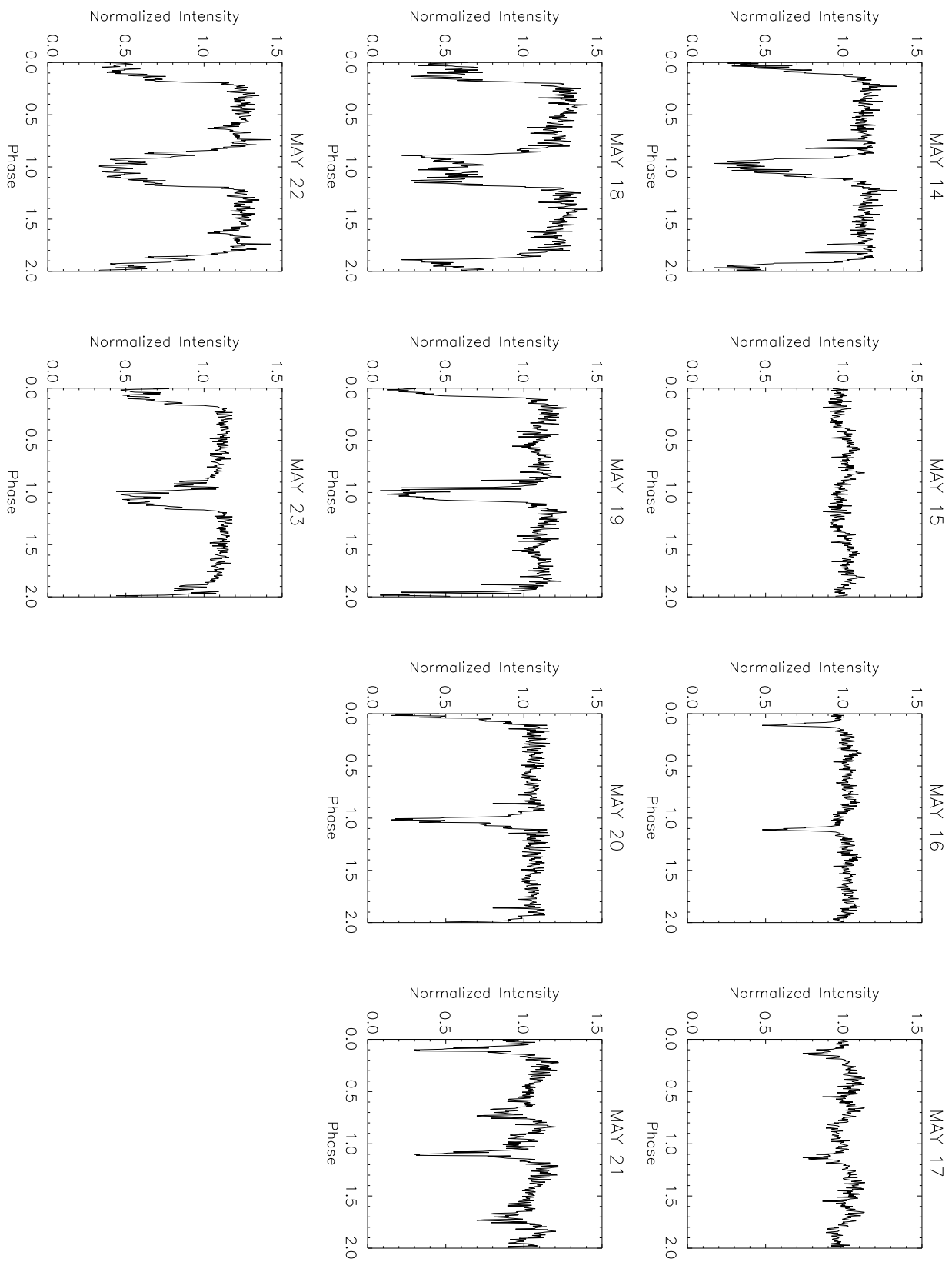


Fig. 6.—

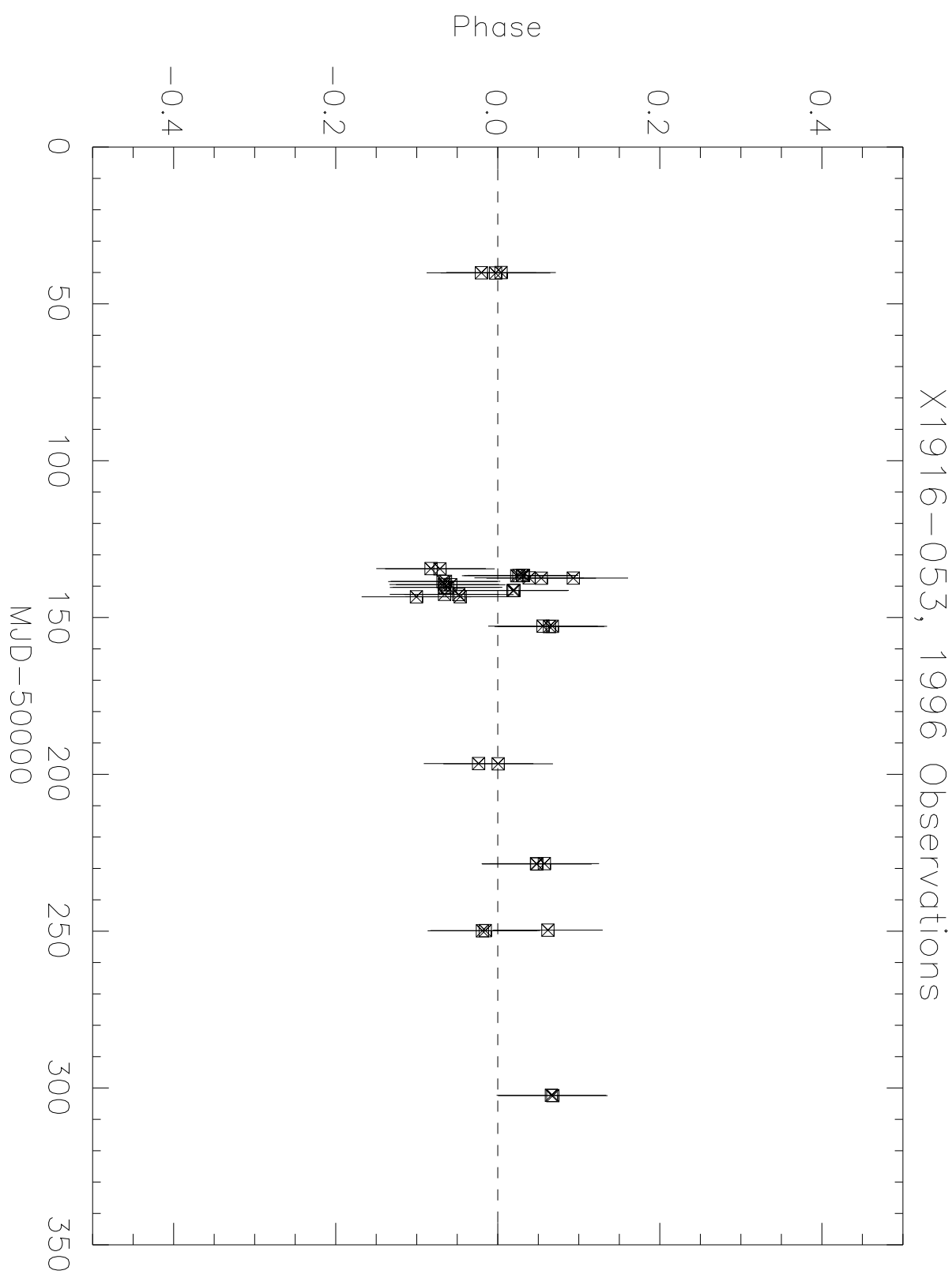


Fig. 7.—

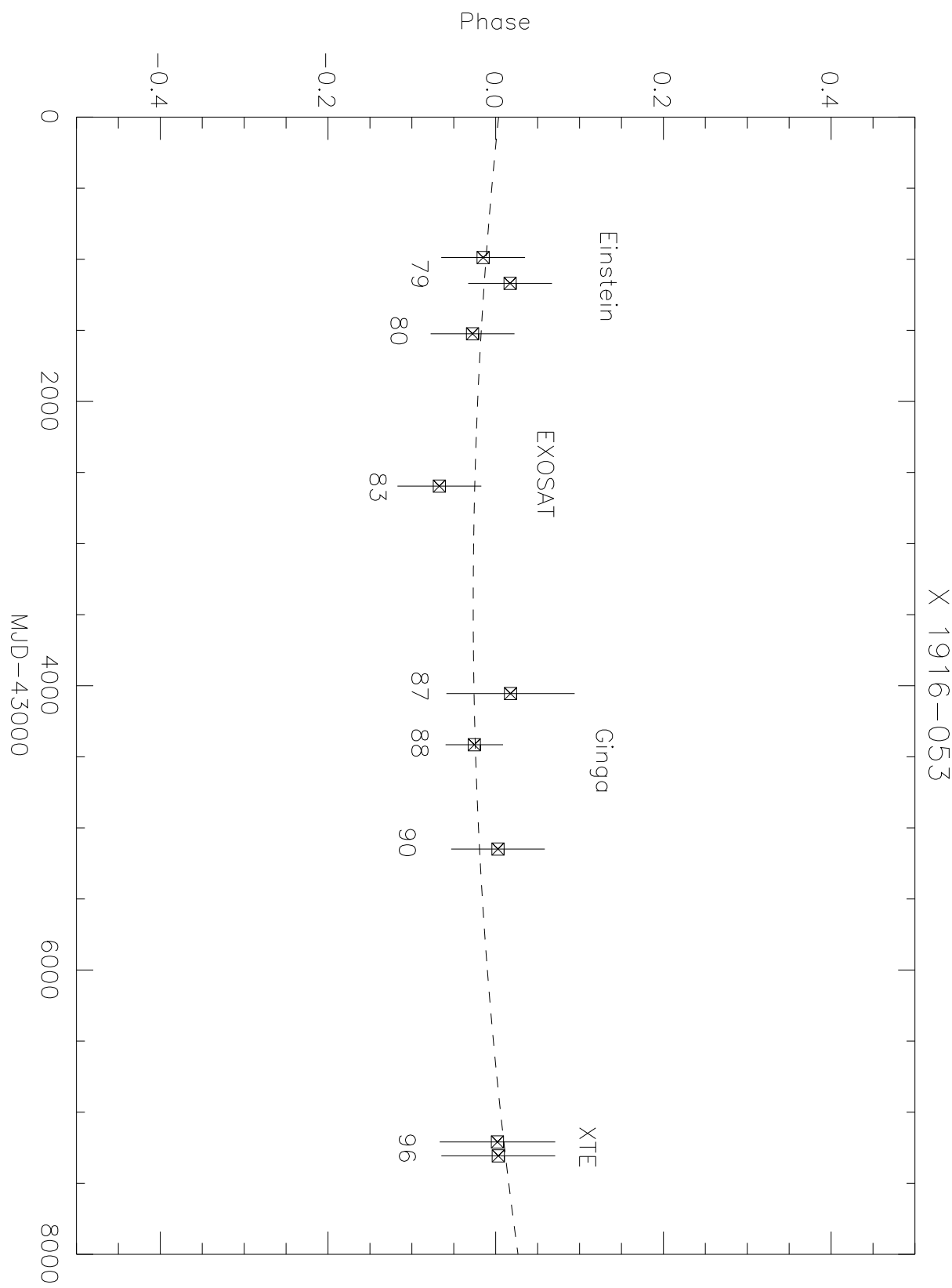


Fig. 8.—

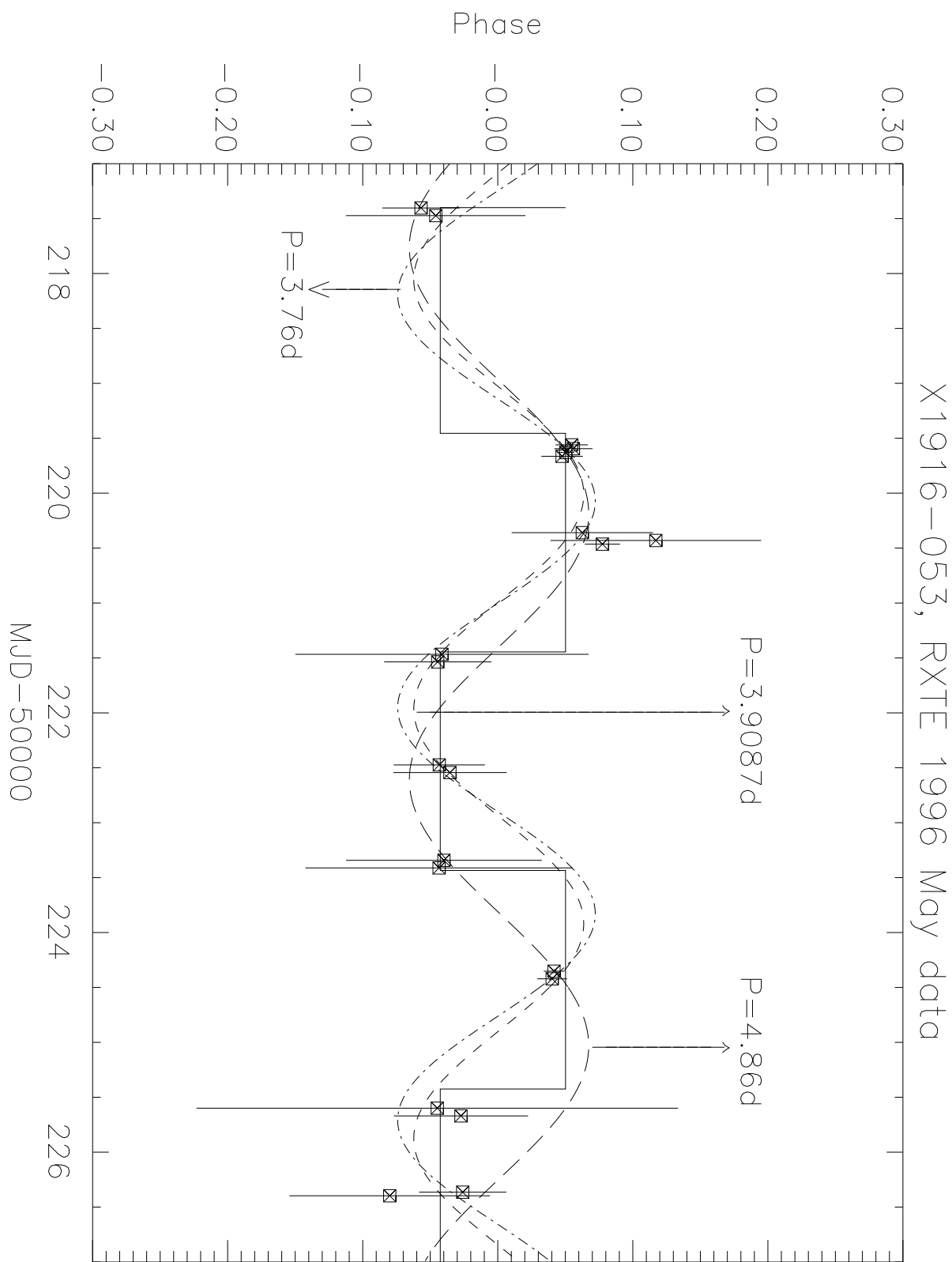


Fig. 9.—

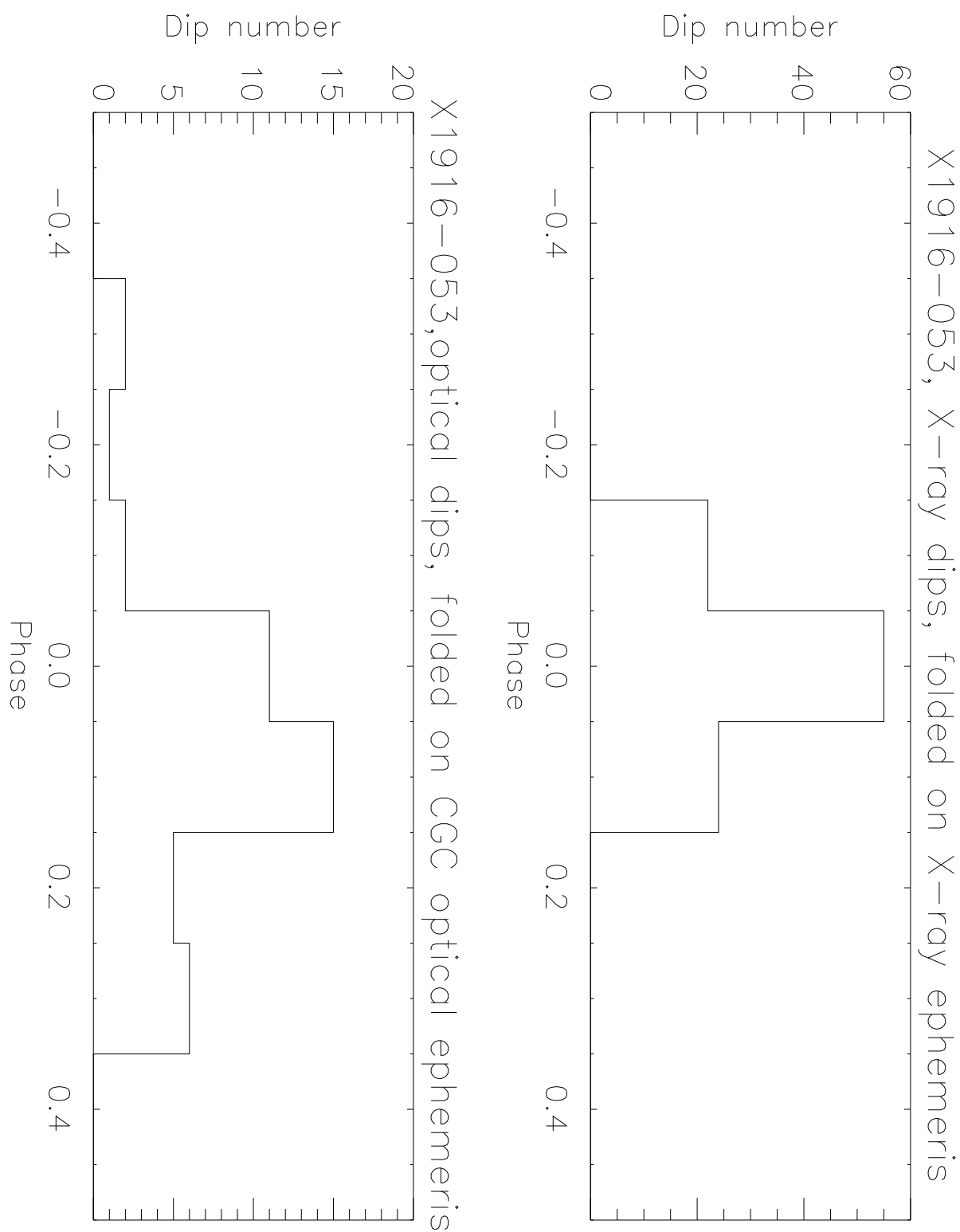


Fig. 10.—

X1916-053, 87-96 optical observations

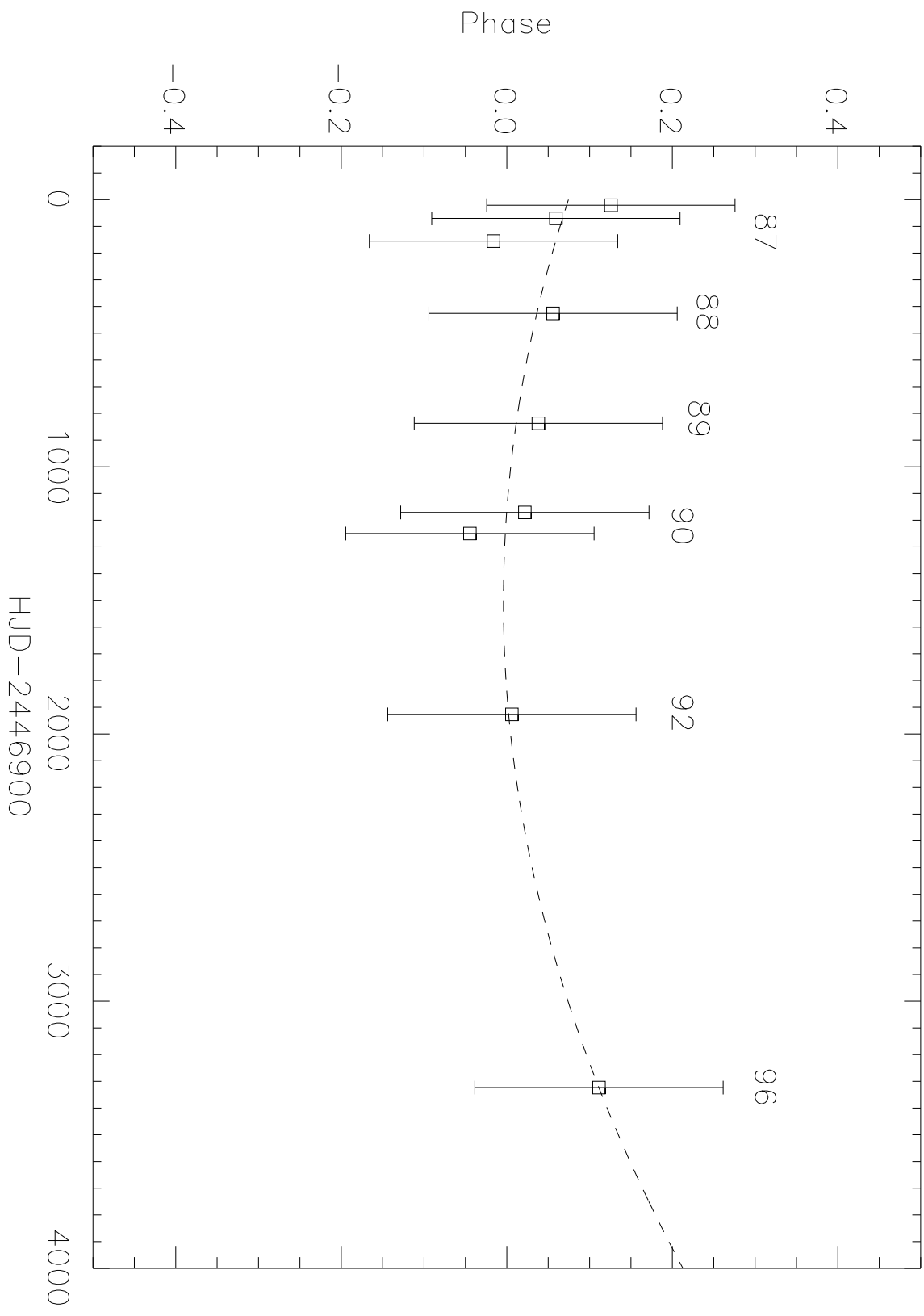


Fig. 11.—

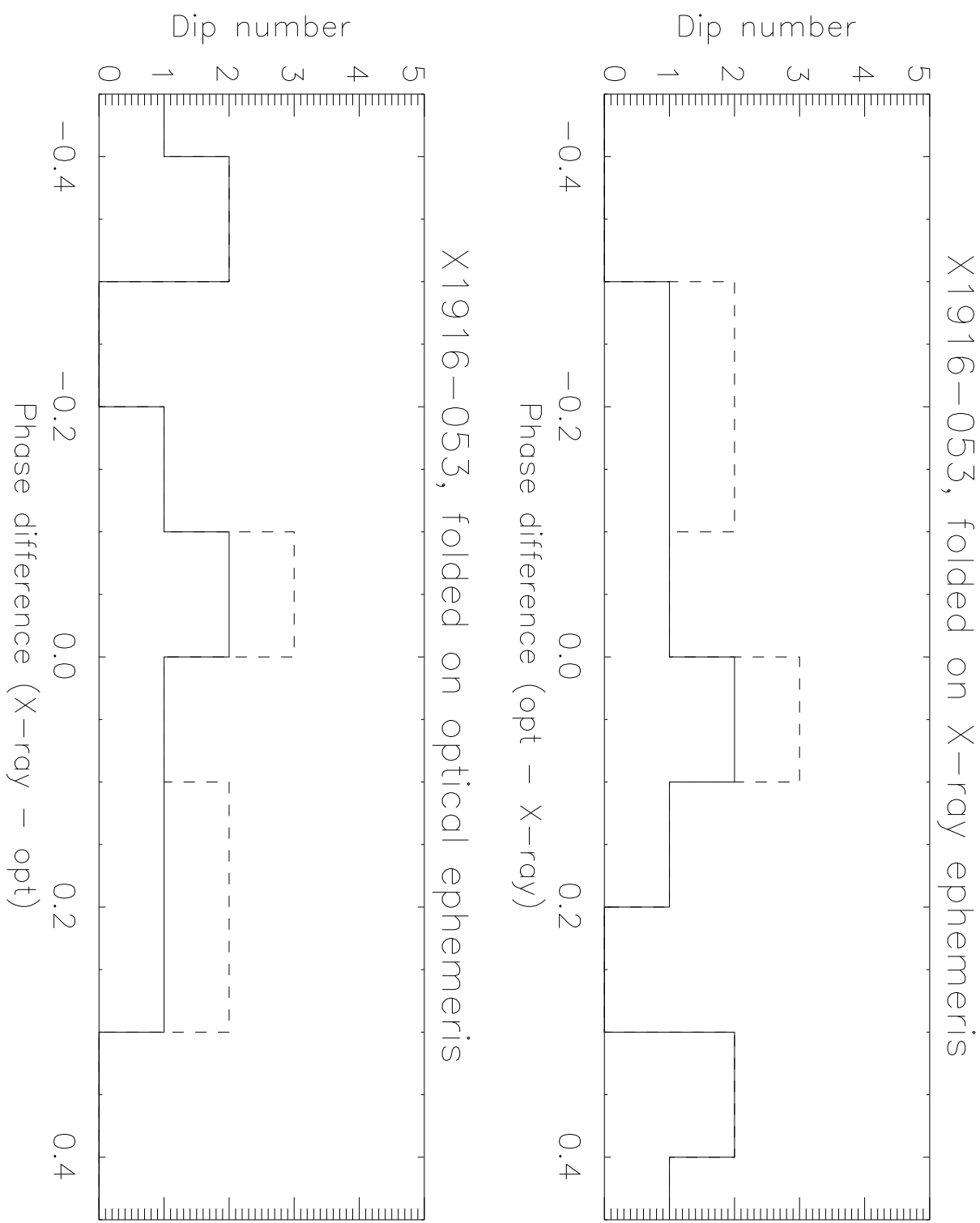


Fig. 12.—

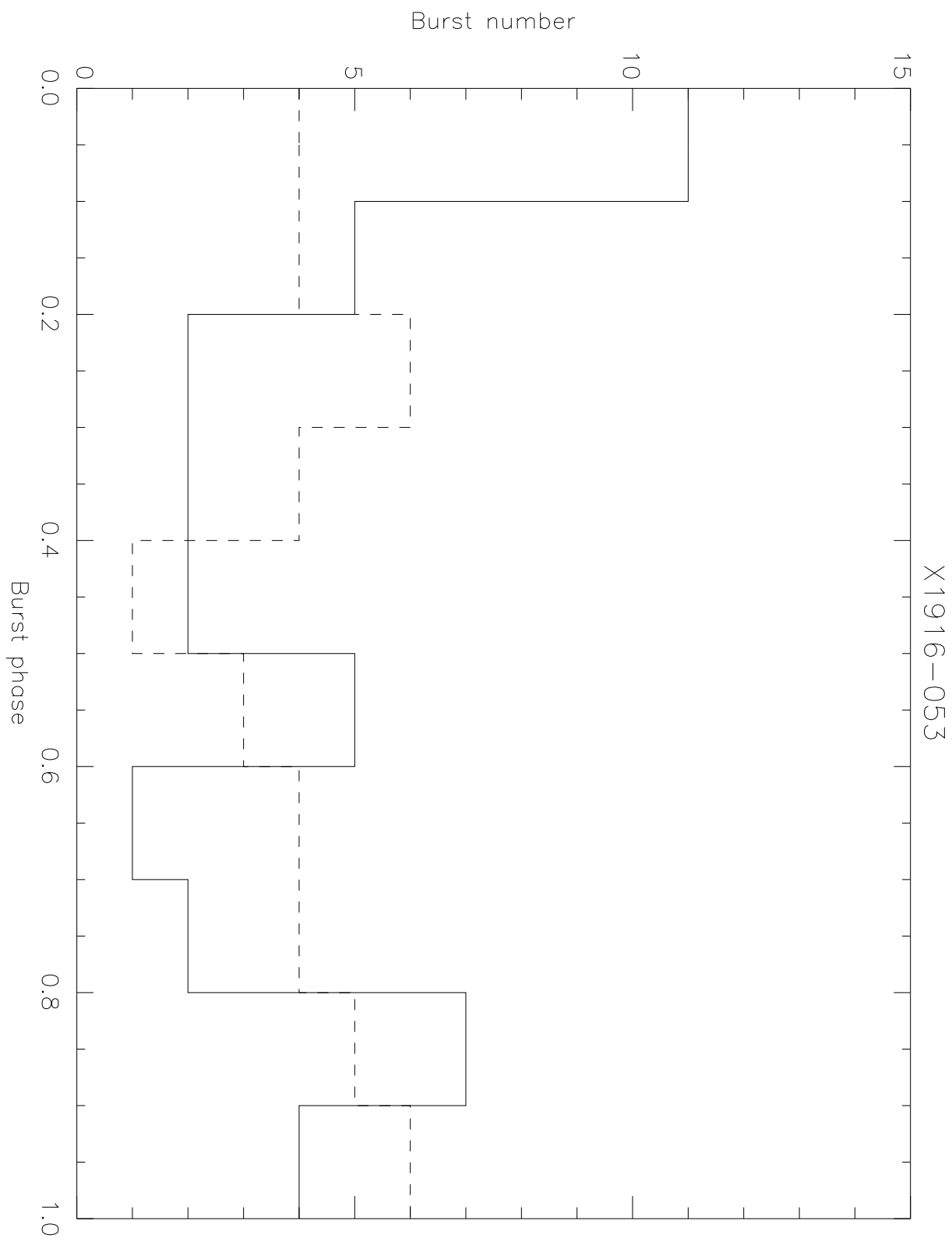


Fig. 13.—